ELSEVIER

The SARS coronavirus spike glycoprotein is selectively recognized by lung surfactant protein D and activates macrophages

Rikke Leth-Larsen[a,b], Fei Zhong[a,b], Vincent T.K. Chow[a], Uffe Holmskov[d], Jinhua Lu[a,b,c,*]

[a]Department of Microbiology, National University of Singapore, Singapore 117597, Singapore
[b]National University Medical Institute, National University of Singapore, Singapore 117597, Singapore
[c]Immunology Program, Faculty of Medicine, National University of Singapore, Singapore 117597, Singapore
[d]Medical Biotechnology Center, Institute of Medical Biology, University of Southern Denmark, Winsloewparken 25, DK-5000 Odense C, Denmark

Abstract

The severe acute respiratory syndrome coronavirus (SARS-CoV) infects host cells with its surface glycosylated spike-protein (S-protein). Here we expressed the SARS-CoV S-protein to investigate its interactions with innate immune mechanisms in the lung. The purified S-protein was detected as a 210 kDa glycosylated protein. It was not secreted in the presence of tunicamycin and was detected as a 130 kDa protein in the cell lysate. The purified S-protein bound to Vero but not 293T cells and was itself recognized by lung surfactant protein D (SP-D), a collectin found in the lung alveoli. The binding required Ca^{2+} and was inhibited by maltose. The serum collectin, mannan-binding lectin (MBL), exhibited no detectable binding to the purified S-protein. S-protein binds and activates macrophages but not dendritic cells (DCs). It suggests that SARS-CoV interacts with innate immune mechanisms in the lung through its S-protein and regulates pulmonary inflammation.
© 2006 Elsevier GmbH. All rights reserved.

Keywords: Dendritic cells; Macrophages; MBL; SARS-CoV; SP-A; SP-D

Introduction

Severe acute respiratory syndrome (SARS), which is highly transmissible via the respiratory route and is associated with significant mortality, has been attributed to pulmonary infection with a novel coronavirus (SARS-CoV) (Drosten et al., 2003; Fouchier et al., 2003; Ksiazek et al., 2003; Kuiken et al., 2003). Coronaviruses are positive-stranded RNA viruses with genomes of ~30 kb in size (Enjuanes et al., 2001). Sequencing of its genome shows that SARS-CoV expresses the spike (S), envelope (E), membrane (M) and nucleocapsid (N) proteins (Drosten et al., 2003; Fouchier et al., 2003; Ksiazek et al., 2003; Kuiken et al., 2003). S-proteins are expressed on the surface of CoVs to mediate virus–host cell interactions leading to host cell infection (Cavanagh et al., 1986; Luo et al., 1999; Gallagher and Buchmeier, 2001). An important

property of S-protein is the high degree of glycosylation (Cavanagh, 1995). Whether and how the carbohydrate structures on S-proteins benefit the virus are unclear. Lectins that recognize microbial carbohydrate structures and target microbes for destruction and clearance (Weis et al., 1998), form an important arm of host innate immunity and it is possible that the highly glycosylated S-protein is recognized by such lectins.

The collectins are multimeric molecules assembled from identical or similar polypeptides and are a group of host lectins that recognize a wide range of microbial pathogens (Lu et al., 2002; Holmskov et al., 2003). Each collectin polypeptide is composed of a middle collagen-like region flanked by an N-terminal cycteine-rich segment and an α-helical neck region that links the C-terminal Ca^{2+}-dependent carbohydrate-recognition domain to the collagen-like region (CRD) (Lu et al., 2002; Holmskov et al., 2003). Three polypeptides form a collagen-like triple helix in the middle of the molecule and the neck region bundles the C-terminal CRDs into clusters of three. These trimeric structures are further assembled through disulfide formation at the N-terminal segments to form the different collectin molecules (Lu et al., 2002; Holmskov et al., 2003). Thus assembled collectin molecules display clustered CRDs at the periphery which, as shown by electron microscopy, can afford dimensions and flexibility to achieve multivalent binding to sugar residues on microbial pathogens (Voss et al., 1988; Lu et al., 1990, 1993, 2002; Holmskov et al., 1995, 2003). Three collectins are well-characterized in man, i.e. mannan-binding lectin (MBL), surfactant protein A (SP-A) and D (SP-D) (Lawson and Reid, 2000; Crouch and Wright, 2001; Jack et al., 2001). MBL is found predominantly in the blood circulation whereas SP-A and SP-D are expressed mainly in the lung at the alveolar surface associated with the surfactant monolayer (Lawson and Reid, 2000; Crouch and Wright, 2001; Jack et al., 2001). SP-A and SP-D are also found in extra-pulmonary tissues (Lu, 1997; Madsen et al., 2000).

The importance of these collectins in innate immunity is reflected in immunological disorders associated with collectin deficiencies. MBL-deficiency leads to poor complement activation and defective microbial opsonization for phagocytosis during childhood (Super et al., 1989). MBL$^{-/-}$ mice exhibit higher mortality compared with wild type mice upon *Staphylococcus aureus* challenge (Shi et al., 2004). Compared with wild type mice, SP-A$^{-/-}$ mice exhibit decreased killing of *B. streptococcus* and *Haemophilus influenzae*, display elevated lung inflammation as well as decreased oxidant production and macrophage phagocytosis (LeVine et al., 2000). SP-D$^{-/-}$ mice show increased lung inflammation and oxidant production but decreased macrophage phagocytosis (LeVine et al., 2000). Deficiency in either SP-A or SP-D expression leads to increased inflammation and reduced pathogen uptake by alveolar macrophages. The latter is consistent with that both pulmonary collectins and the serum collectin MBL promote pathogen uptake by macrophages (LeVine et al., 2000; Kudo et al., 2004). In the present study, we investigated whether the lung collectins are able to recognize the SARS-CoV S-protein.

Methods

Cells and reagents

Vero African green monkey kidney cells and HEK293T human embryonic kidney cells (ATCC, Rockville, MD, USA) were cultured in medium 199 (Sigma M0393) and Dulbecco's modified Eagle's medium (DMEM), respectively, supplemented with 10% (v/v) fetal bovine serum, 100 U/ml of penicillin and 100 μg/ml streptomycin at 37 °C and 5% CO_2. Medium 199 was further supplemented with 10 mM L-glutamine. SP-D was purified from amniotic fluid as described previously (Strong et al., 1998; Leth-Larsen et al., 2003). The mouse monoclonal (clones hyb 245-01, hyb 245-02 and hyb 246-4) and rabbit polyclonal SP-D antibodies were as described (Madsen et al., 2000). Biotinylated mouse anti-human MBL antibody (131-1, Immunolex) was kindly provided by S. Thiel, Aarhus University, Denmark. An anti-human angiotensin-converting enzyme 2 (ACE2) monoclonal antibody was purchased from Alpha Diagnostic (San Antonio, TX, USA).

Expression vectors

The full-length synthetic SARS-CoV S-protein cDNA, in the pcDNA3.1 expression vector, was kindly provided by Michael Farzan (Brigham and Women's Hospital, Harvard, Boston, USA) (Li et al., 2003). The vector was modified to express the surface domain as a secreted trimeric protein (Fig. 1). Briefly, a *Hin*d III site was introduced in the S-protein expression vector between the surface and the transmembrane domains (corresponding to residues K_{1193} and W_{1194}; accession no. NC_004718), using the QuikChang XL Site-Directed Mutagenesis Kit (Stratagene, La Jolla, CA, USA) and the following primer pair (5′–3′): GTA CGA GCA GTA CAT CAA GCT TCC TTG GTA TGT GTG GCT G/CAG CCA CAC ATA CCA AGG AAG CTT GAT GTA CTG CTC GTA C. The plasmid was then digested with *Hin*d III and dephosphorylated.

A parent pcDNA-SPD/MH vector was constructed as follows: A cDNA fragment encoding 25 residues (V_{194}ASLRQQVEALQGQVQHLQAAFSQY$_{218}$, accession no. NM_003019), corresponding to the neck region of human SP-D, was amplified from the human SP-D cDNA (Lu et al., 1992) by PCR using the following
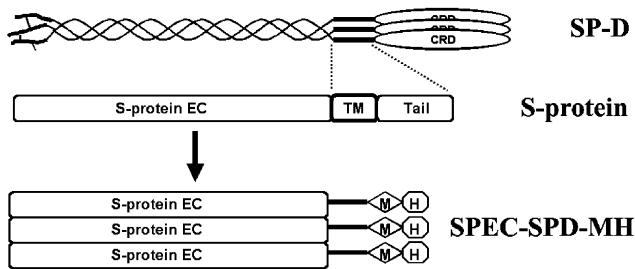
Fig. 1. Expression of S-protein trimers. A single SP-D polypeptide consists of four distinct regions and the 'neck' region is a 25 amino acid segment (V_{194}-Y_{218}, NM_003019) that forms triple coiled-coils. S-protein has a large extramembrane domain (S-protein EC), a transmembrane domain (TM) and a short intramembrane tail (Tail). To express S-protein EC as a trimer, the TM and Tail domains in S-protein was replaced by the 25-residue SP-D 'neck' sequence which was followed by a C-terminal myc and His tag (SPEC-SPD-MH). This hybrid protein is expected to form trimers.

primer pair (5′–3′): GCT CTA GAG TTG CTT CTC TGA GGC AG/GAA GGG CCC ATA CTG AGA GAA AGC AGC CT. The DNA fragment was cloned into the *Xba* I/*Apa* I site of the pcDNA3.1 myc-His vector (Invitrogen, San Diego, CA, USA) to generate the pcDNA-SPD/MH vector that encodes the SP-D sequence in fusion with C-terminal myc/His sequences.

A PCR product encoding the SP-D and myc/His (SPD-myc/His) sequences was amplified from the pcDNA3.1-SPD/MH vector using the following primer pair (5′–3′): TTG CCC AAG CTT GTT GCT TCT CTG AGG CAG C/TTG CCC AAG CTT TCA ATG GTG ATG GTG ATG ATG and digested with *Hin*d III and ligated into the *Hin*d III-digested S-protein expression vector to generate the pSPSD-SPD/MH expression vector.

Protein expression and purification

Approximately 4×10^6 293T cells were seeded in a T75 flask and cultured overnight and the medium was replaced with 10 ml fresh medium for 1 h. 25 μg of the pSPSD-SPD/MH vector in 0.4 ml water was slowly mixed with 0.1 ml of 2.5 M CaCl$_2$ and then slowly mixed with 0.5 ml of 2× HBS buffer (280 mM NaCl, 10 mM KCl, 1.5 mM NaH$_2$PO$_4$, 12 mM dextrose, 42 mM HEPES, pH 7.05). The DNA mixture was vortexed and incubated for 1 min before adding to the 293T cells. After 6 h, the cells were washed in PBS and then cultured in serum-free DMEM containing BSA (0.1 mg/ml) for 72 h. The medium was mixed overnight with Ni-NTA-agarose (Qiagen). After washing, bound proteins were eluted with imidazole following the manufacturer's instructions. In some experiments, 293T cells that were transfected with pSPSD-SPD/MH and cultured as

above except that the cells were cultured for 36 h in the presence or absence of tunicamycin (10 μg/ml). The medium was mixed with Ni-NTA-agarose and then precipitated. Bound proteins were eluted with imidazole. The cellular fractions were lysed in lysis buffer (20 mM Tris, pH 7.4, 150 mM NaCl, 1 mM EDTA, 1 mM EGTA, and 1% (v/v) Nonidet P-40 and complete protease inhibitor cocktail (Roche)). The lysates were clarified by centrifugation and the supernatants, together with the imidazole eluate from Ni-NTA-agarose, were subjected to SDS-PAGE on 7.5% (w/v) gels. The separated proteins were electroblotted and detected by Western blotting using a mouse anti-myc antibody followed by a goat anti-mouse IgG conjugated with alkaline phosphatase. The blots were developed using the Immun-Star^{TM} substrate pack (Bio-Rad).

Biotinylation and precipitation of cell surface proteins

293T and Vero cells (2×10^6) were washed 3 times with ice-cold PBS (pH 8.0) and re-suspended in 0.1 ml of PBS. The cells were incubated for 30 min with 50 μg of EZ-Link^{TM} Sulfo-NHS-LC-Biotin (Pierce). After addition of Tris (pH 8.0) to 50 mM, the cells were washed 3 times in ice-cold PBS (pH 8.0) and lysed in 0.1 ml of lysis buffer. The lysate was cleared by centrifugation and then incubated with a 50% slurry of the streptavidin-Sepharose beads (Pierce) (40 μl). The beads were harvested and, after washing 3 times in the lysis buffer, bound proteins were eluted in the SDS-PAGE sample buffer. The eluted proteins were separated on 10% (w/v) SDS-PAGE gels and ACE2 was detected by Western blotting.

Binding of SP-D to purified S-protein

Polystyrene microtiter plates (Maxisorp, Nunc, Roskilde, Denmark) were coated with purified S-protein (5 μg/ml) overnight at 4 °C in 50 mM sodium carbonate buffer (pH 9.6) and then washed 4 times with Tris-buffered saline (TBS) (20 mM Tris and 150 mM NaCl, pH 7.4) containing 0.05% (v/v) Tween 20 and 5 mM CaCl$_2$. Plates were incubated with the washing buffer for 15 min at room temperature for blocking. A series of two-fold dilutions of purified human SP-D was made in the washing buffer (5 μg/ml to 0) and incubated with the coated plates overnight at 4 °C. In some experiments, SP-D was diluted to 5 μg/ml in the washing buffer containing different concentrations of maltose (0–100 mM) or 10 mM *N*-acetyl-D-glucosamine (GlcNAc), mannose or galactose. SP-D was also diluted in TBS containing 0.05% (v/v) Tween 20 and 10 mM EDTA. The plates were washed and then incubated with monoclonal (2 μg/ml) or polyclonal (10 μg/ml) SP-D

antibodies, respectively, for 2 h with shaking. After washing, the plates were incubated with alkaline phosphatase-conjugated goat anti-mouse or goat anti-rabbit IgG (1:1000 dilutions; Bio-Rad, Hercules, CA, USA) for 1 h with shaking. The plates were, after washing, developed using *para*-nitrophenyl phosphate (1 mg/ml) dissolved in substrate buffer (0.1 M Tris, 5 mM $MgCl_2$, 0.1 M NaCl, pH 9.5). The plates were read by spectrophotometry at 405 nm. Experiments were carried out in duplicates.

Binding of MBL to mannan and S-protein

Microtiter plates were coated with Baker's yeast mannan (Sigma, St. Louis, MI, USA), S-protein, or BSA as described above at 5 µg/ml. The wells were blocked in BSA (1 mg/ml in TBS) for 1 h and then incubated overnight at 4 °C with human serum diluted to 5% (v/v) at the highest concentration followed by 3.5-fold dilutions in MBL binding buffer (20 mM Tris, 10 mM $CaCl_2$, 0.1% (w/v) BSA, 1 M NaCl and 0.05% (v/v) Triton X-100, pH 7.4). After washing in the MBL binding buffer, the plates were incubated with biotiny-lated anti-MBL monoclonal antibody (1:2500) for 2 h with shaking. The plates were incubated with alkaline phosphatase-conjugated streptavidin (1 µg/ml in TBS containing 0.05% (v/v) Tween 20 and 5 mM $CaCl_2$) for 1 h with shaking. The plates were, after washing, developed with *para*-nitrophenyl phosphate (1 mg/ml) and read by spectrophotometry at 405 nm. Experiments were carried out in duplicates.

Flow cytometry

Macrophages and dendritic cells (DCs) were cultured from isolated human monocytes as previously described (Cao et al., 2006). Macrophages, DCs, 293T and Vero cells were harvested, incubated for 30 min with 20% (v/v) goat serum, and then stained for 45 min on ice with a mouse monoclonal anti-ACE2 antibody. After wash-ing, the cells were further stained for 30 min with goat anti-mouse IgG (RPE). The cells were after washing, fixed in 1% (w/v) paraformaldehyde in PBS (pH 7.6) and then analyzed on a FACScalibur using the CellQuest software (BD Biosciences). To examine possible DC and macrophage activation by S-protein, the cells were stimulated with purified S-protein (20 µg/ml) or, as a control, lipopolysaccharide (LPS) for 6 h in the presence of brefeldin A (10 µg/ml). The cells were fixed for 10 min in 1% (w/v) paraformaldehyde and permea-bilized for 15 min with 0.2% (w/v) saponin before blocking and staining with an anti-TNF-α antibody (RPE) or, as a control, an isotype mouse IgG. The cells were analyzed by flow cytometry.

ELISA

DCs and macrophages were stimulated in 96-well plates at 1×10^5/well with purified S-protein (20 µg/ml) or, as a control, LPS (0.5 µg/ml) for 24 h and the supernatants were analyzed using the DuoSet ELISA Development kits for TNF-α, IL-6 and IL-8 (R&D Systems Inc., McKinley Place N.E., MN). The experi-ments were performed in triplicate and results were presented as means ± SD.

S-protein binding to the cell surface

The Vero and 293T cells were detached with 0.5 mM EDTA in PBS, washed and re-suspended in PBS contain-ing 0.5% (w/v) BSA (PBS-BSA) at $\sim 4 \times 10^7$/ml. The cells (50 µl each) were each incubated with 2.5 µg of S-protein for 2 h at 4 °C with rotation. The cells were washed in PBS-BSA and incubated in 20% (v/v) goat serum in PBS-BSA for 30 min on ice. After washing in cold PBS-BSA, the cells were incubated with a mouse anti-myc antibody (Roche, Indianapolis, IN, USA) at 10 µg/ml for 30 min on ice. As a control, the cells were incubated with isotype mouse IgG1. After washing in PBS-BSA, the cells were incubated with goat F(ab')₂ anti-mouse IgG conjugated with RPE for 40 min on ice. The cells were washed and fixed in 1% (w/v) paraformaldehyde and analyzed on a FACScalibur flow cytometer (BD Biosciences). DCs and macrophages were harvested and examined for S-protein binding as above.

In some experiments, S-protein (10 µg/ml) was pre-incubated overnight at 4 °C with SP-D (40 µg/ml) or BSA (40 µg/ml) in TBS containing 2 mM $CaCl_2$ before incubation with Vero cells in TBS containing 0.5% (w/v) BSA and 2 mM $CaCl_2$. Cells were washed twice with the binding buffer and then incubated with the myc antibody followed by goat anti-mouse IgG and analyzed by flow cytometry as above.

Results

Expression of SARS-CoV S-protein

In coronavirus, the S-proteins are anchored to the lipid envelope like a type I receptor and contains 3 domains, i.e. a large N-terminal surface domain, a single transmem-brane domain, and a short C-terminal domain located inside the envelope (Cavanagh, 1995). S-protein mediates coronavirus interaction with host cells leading to cellular infection. S-protein is the predominant surface protein on SARS-CoV and is potentially a major viral surface structure recognized by the host innate immune mechan-isms. Investigation of S-protein interaction with host cells helps in the identification of mechanisms by which SARS-CoV interacts with the hosts.

To express the SARS-CoV S-protein as a soluble probe, an expression vector was constructed in which sequences encoding the transmembrane and C-terminal domains of the S-protein were deleted by introducing a *Hin*d III restriction site immediately upstream of the transmembrane domain (Fig. 1). This surface domain of S-protein was expressed as a trimer for two main reasons: to reflect the multiplicity of S-protein on the virus and to increase the affinity of the S-protein probe or the sensitivity of the S-protein binding assays. S-protein trimerization was engineered by C-terminal fusion with a sequence derived from the 'neck' region of human lung surfactant protein D (SP-D) (Fig. 1). This 'neck' sequence forms stable triple coiled-coil structures which have been shown in SP-D and MBL to bring the CRDs together as clusters of three (Hoppe et al., 1994; Weis and Drickamer, 1994). The 'neck' sequence was linked to myc and His tag sequences to facilitate purification and detection of the expressed S-protein (Fig. 1).

S-protein was expressed in 293T cells in serum-free medium and purified using the nickel-based, Ni-NTA-agarose resins that bind to the C-terminal His tags. The purified S-protein migrated as a protein of ~200 kDa on SDS-PAGE under reducing conditions and was recognized by an anti-myc antibody (Fig. 2). The size of the purified S-protein under reducing conditions is consistent with that reported in a previous study (Li et al., 2003). However, it is much larger than the predicted molecular mass of ~130 kDa (1194 residues). Like other coronavirus S-proteins, the SARS-CoV S-protein is also characterized by a large number of potential Asn-linked glycosylation sites, i.e. 18 sites on the surface domain (Drosten et al., 2003; Fouchier et al., 2003; Ksiazek et al., 2003; Kuiken et al., 2003). As shown in Fig. 2B,

Asn-linked glycosylation contributes substantially to the observed increase in molecular mass of S-protein. Expression of S-protein in the presence of tunicamycin, an inhibitor of Asn-linked glycosylation, blocked the secretion of S-protein to the culture media; S-protein could not be isolated from the media of these cells (Fig. 2B, lane 2). However, when the cell lysate was examined by Western blotting, S-protein was detected in these tunicamycin-treated cells as a protein of ~130 kDa (Fig. 2B, lane 4). In contrast, S-protein detected in the lysate of transfected 293T cells, which were not treated with tunicamycin, remained ~200 kDa (Fig. 2B, lane 3). This indicated that the reduction in the size of S-protein in the tunicamycin-treated cells was due to loss of Asn-linked glycosylation which also prevented its functional maturation and secretion.

S-protein binds to Vero but not 293T cells

Previous studies have shown that Vero cells, but not 293T cells, are permissive to SARS-CoV infection and that the SARS-CoV receptor ACE2 is expressed on Vero but not 293T cells (Li et al., 2003). This was also observed in this study, i.e. Vero but not 293T cells express surface ACE2 (Fig. 3A). To examine whether S-protein expressed in this study is recognized by ACE2, Vero cells were incubated with the purified S-protein and bound S-protein was detected by flow cytometry using a myc antibody. S-protein showed prominent binding to Vero cells but no binding to 293T cells was observed (Fig. 3B). These results are consistent with the reported S-protein binding to Vero but not 293T cells (Li et al., 2003). In the same report, inhibition of S-protein binding to Vero cells by soluble ACE2 was observed suggesting S-protein binding to ACE2 on Vero cells.

SARS-CoV S-protein is recognized by SP-D

The collectins are a large family of host lectins that recognize carbohydrate structures on a wide range of microbial pathogens to activate host innate immunity (Lu et al., 2002; Holmskov et al., 2003). The heavily glycosylated nature of the SARS-CoV S-protein prompted us to examine whether it is recognized by these host lectins. The lung alveoli represent the primary host interface with SARS-CoV. Two important arms of host innate immunity are present at the air–epithelial interface of lung alveoli, i.e. the lung surfactant proteins (SP-A and SP-D) and alveolar macrophages. Hence, the interaction between S-protein and SP-D was investigated. SP-D selectively recognizes maltose and mannose residues on microbes but shows little affinity for GlcNAc (Lu et al., 1992). Purified S-protein was immobilized on 96-well plates and incubated with human SP-D. Bound SP-D was detected with a mouse
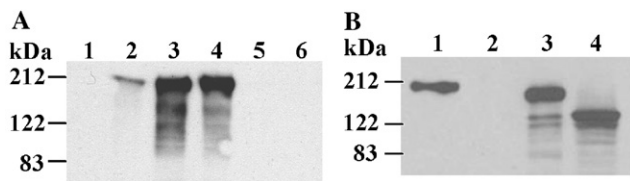

Fig. 2. Expression and purification of S-protein: (A) The SPEC-SPD-MH protein was expressed in 293T cells and purified on Ni-NTA-agarose and eluted with imidazole. The protein was eluted in 6 fractions (1–6), and upon separation on 7.5% SDS-PAGE gels, analyzed by Western blotting using an anti-myc antibody. (B) 293T cells transfected with pSPSD-SPD/MH and cultured for 36 h in the absence (lanes 1 and 3) or presence (lanes 2 and 4) of tunicamycin (10 μg/ml). The media were mixed with Ni-NTA-agarose, bound proteins were precipitated and eluted with imidazole (lanes 1 and 2). The cell pellets were lysed and, upon centrifugation, the supernatants (lanes 3 and 4), together with proteins precipitated from the media (lanes 1 and 2) were separated on 10% (w/v) SDS-PAGE gels. The separated proteins were analyzed by Western blotting using a mouse anti-myc antibody.
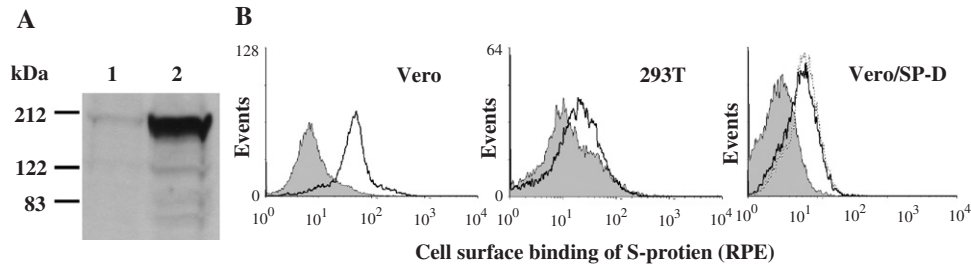
Fig. 3. Binding of S-protein to 293T and Vero cells: (A) 293T (1) and Vero (2) cells were washed and then surface biotinylated. The cell lysates were incubated with streptavidin-Sepharose to precipitate biotinylated surface proteins which were subjected to Western blotting using the anti-ACE2 antibody. (B) Vero and 293T cells were detached with 0.5 mM EDTA in PBS, washed and then incubated with purified S-protein. After washing, the cells were incubated with a mouse anti-myc antibody (solid lines). As controls, the cells were not incubated with S-protein but stained with the same antibodies (solid histograms). In another experiment (Vero/SP-D), S-protein was also incubated with human SP-D (dotted line) or, as a control, with BSA (solid line), before incubation with Vero cells and bound S-protein was similarly detected by flow cytometry using the anti-myc antibody. The solid histogram in this experiment represents signals detected on cells that were not incubated with S-protein but stained with the anti-myc antibody.

monoclonal anti-SP-D antibody or a rabbit polyclonal anti-SP-D antibody. As shown in Fig. 4A, SP-D was shown to bind to immobilized S-protein in a dose-dependent manner. Binding was detectable at ~150 ng/ml SP-D and approached saturation at 625 ng/ml SP-D. The binding was completely blocked in the presence of 10 mM EDTA implying that the CRDs of SP-D, which require Ca^{2+} to bind to selected sugar ligands, was involved (Fig. 4A).

To further examine whether SP-D binds to the carbohydrate moiety on S-protein, the binding assay was also carried out in the presence of maltose, the major sugar residue recognized by SP-D. At maltose concentrations of 12.5 mM or higher, SP-D binding to S-protein was completely blocked (Fig. 4B). At concentrations between 1.5 and 6.25 mM, maltose showed dose-dependent inhibition of SP-D binding to S-protein. Therefore, binding of SP-D to S-protein clearly involves the SP-D CRDs and the carbohydrate structures on S-protein. Although the purified S-protein contains the SP-D 'neck' sequence and the myc and His tag sequences, there are no potential glycosylation sites on these sequences. The carbohydrate-dependent SP-D binding to S-protein rules out SP-D recognition of these regions. Inhibition by other sugars was also examined. As shown in Fig. 4C, SP-D binding to S-protein was inhibited by mannose as well as maltose. However, it was not significantly inhibited by galactose and GlcNAc. These results further confirm the involvement of SP-D lectin activity in S-protein binding.

SARS-CoV S-protein is not recognized by MBL

We then examined whether the serum collectin MBL recognizes S-protein. While SP-D preferentially binds to maltose and mannose residues, MBL binds mainly to mannose, GlcNAc and fucose (Lu et al., 2002; Holmskov et al., 2003). However, both MBL and SP-D bind to mannan, the carbohydrate component of the yeast cell wall. S-protein or, as controls, yeast mannan or BSA, were immobilized on 96-well plates and then incubated with human serum in serial 3.5-fold dilutions in a Ca^{2+}-containing buffer. The diluted human serum served as a source of MBL. Bound MBL was detected using a biotinylated mouse anti-MBL monoclonal antibody. As shown in Fig. 4D, MBL bound to mannan-coated plates in a dose-dependent manner. As a negative control, it showed no specific binding to BSA (Fig. 4D). MBL showed no detectable binding to immobilized S-protein (Fig. 4D). Therefore, S-protein appears to be selectively recognized by SP-D.

S-protein binds to both macrophages and DCs

Since macrophages form an important arm of alveolar innate immunity against microbial infections, possible interaction between S-protein and macrophages was also examined. As for Vero and 293T cells, binding of S-protein to macrophages and DCs was examined by flow cytometry. Firstly, the two cell types were examined for the expression of the SARS-CoV receptor ACE2. Interestingly, ACE2 was detected on macrophages but not on DCs (Fig. 5A). We then examined S-protein binding to macrophages and DCs. As shown in Fig. 5B, S-protein could bind to macrophages. Although ACE2 was not detected on DCs, S-protein was also shown to bind to DCs with a distinct pattern from macrophages (Fig. 5B). This could involve other DC receptors (Jeffers et al., 2004; Marzi et al., 2004). Pre-incubation of S-protein with SP-D did not inhibit S-protein binding to macrophages indicating that the carbohydrate structures on S-protein are probably not involved in the observed S-protein binding to macrophages. SP-D showed no enhancement of S-protein binding to macrophages. SP-D also showed no inhibition or enhancement to S-protein binding to Vero cells (Fig. 3B, right panel).
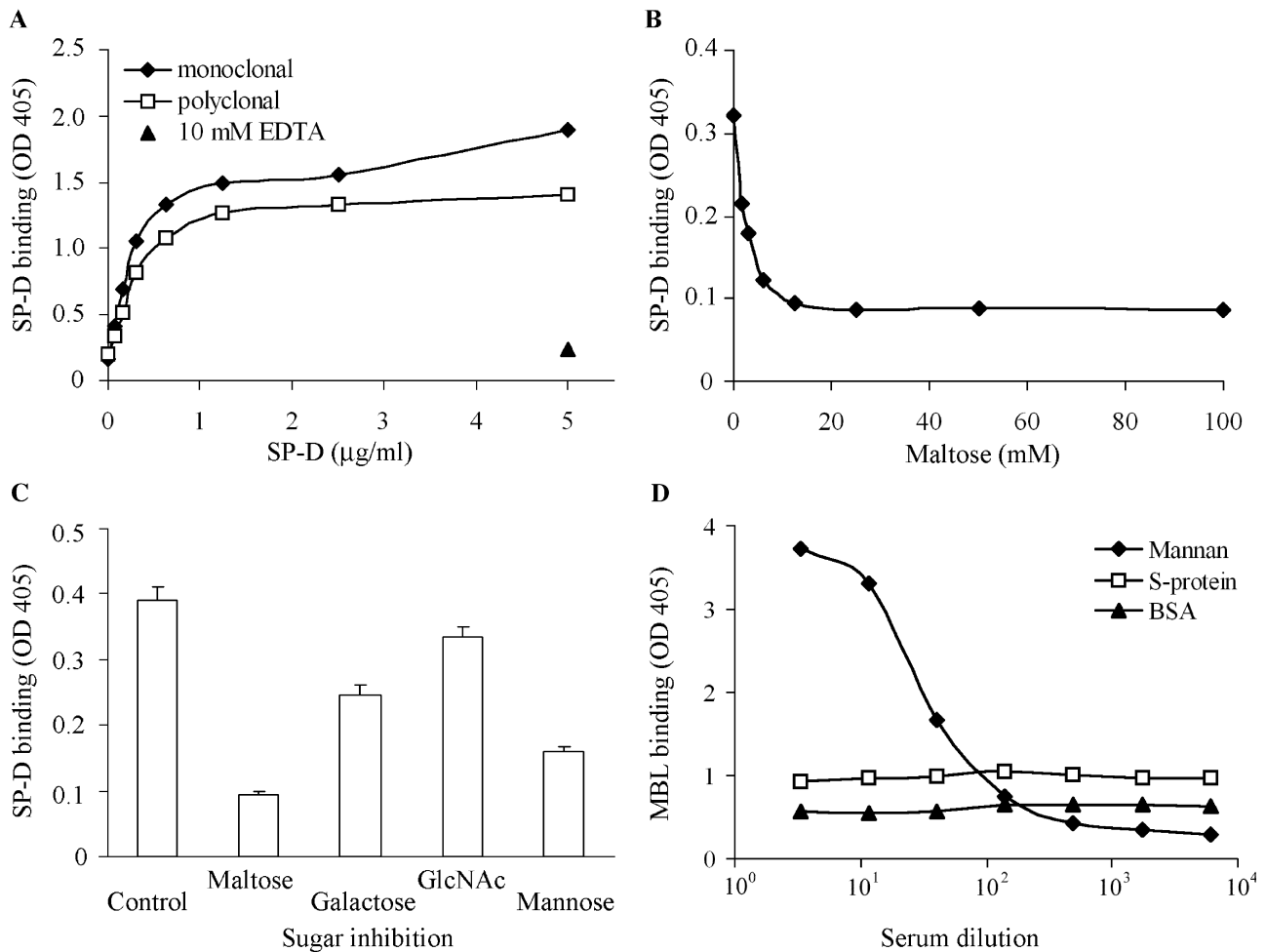
Fig. 4. Binding of SP-D and MBL to S-protein: (A) purified S-protein was coated on 96-well plates (20 μg/ml) and then incubated with purified human SP-D at serial two-fold dilutions in a $CaCl_2$-containing buffer from 5.0 to 0.0375 μg/ml. Bound SP-D was detected by incubation with either a rabbit polyclonal or mouse monoclonal antibody against human SP-D, followed by alkaline phasophatase-conjugated goat secondary antibodies. The plates were developed and then measured at OD405. As controls, SP-D was incubated with S-protein-coated plates in the presence of 10 mM EDTA. The experiments were carried out in duplicate and results were presented as means. (B) S-protein-coated plates were incubated with SP-D at 5 μg/ml in the presence of two-fold dilutions of maltose from 100 to 1.5 mM. The experiments were also performed in duplicate and bound SP-D was detected as above. (C) S-protein-coated plates were incubated with SP-D at 5 μg/ml in the presence of 10 mM maltose, galactose, GlcNAc or mannose. As a control, SP-D was incubated in the absence of sugars. These experiments were carried out in triplicate. (D) 96-well plates were coated with S-protein and, as controls, with yeast mannan or BSA. The plates were then incubated with 3.5-fold dilutions of human sera starting from 5% (v/v) and bound MBL was detected using a biotinylated monoclonal anti-MBL antibody followed by streptavidin-alkaline phosphatase. The experiments were carried out in duplicate and presented as means. The difference in overall OD405 readings between the different experiments reflects the time of incubation after addition of substrate.

However, pre-incubation of S-protein with SP-D increased S-protein binding to DCs. These findings reveal that S-protein binds to macrophages and DCs by distinct mechanisms.

S-protein activates macrophages but not DCs

The effect of S-protein binding to macrophages and DCs was also investigated. The cells were stimulated with S-protein for 6 h in the presence of brefeldin A. The production of tumor necrosis factor-α (TNF-α), a major pro-inflammatory cytokine which is intracellularly retained in the presence of brefeldin A, was examined by flow cytometry. As a positive control, these cells were stimulated with lipopolysaccharide (LPS). As shown in Fig. 5C, macrophages showed TNF-α production upon stimulation with S-protein as well as LPS showing that macrophages were activated by S-protein. DCs were also effectively activated by LPS as shown by the
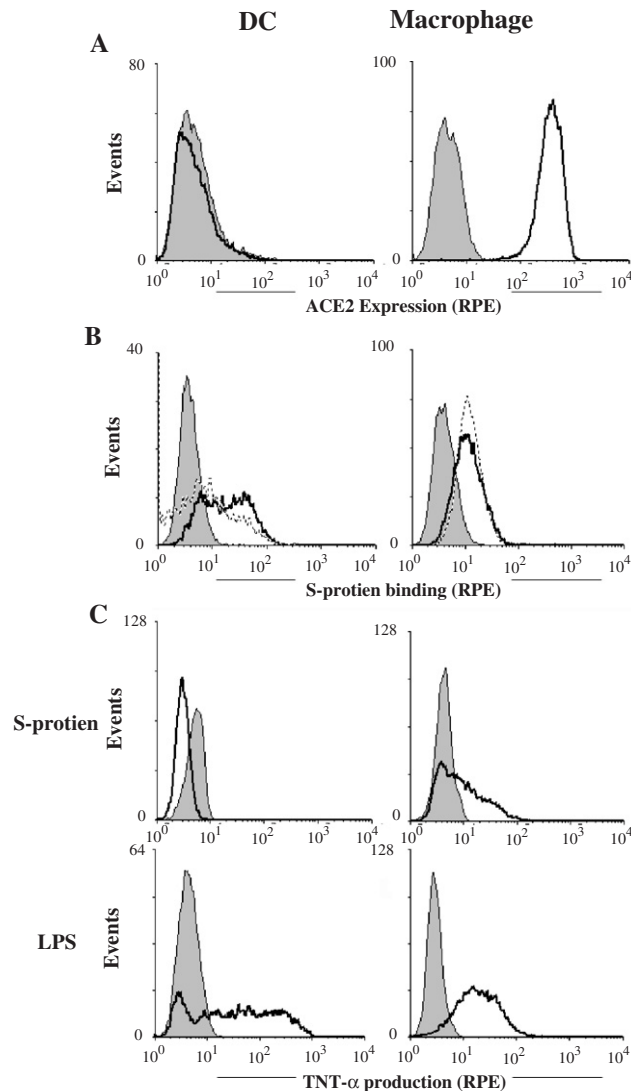
Fig. 5. Binding of S-protein to macrophages and DCs: (A) macrophages and DCs were cultured from monocytes and, upon washing, incubated with a mouse anti-human ACE2 monoclonal antibody (solid lines) or, as a control, isotype IgG (solid histograms). The cells were then incubated with goat (Fab′)₂ anti-mouse IgG (RPE). (B) Macrophages and DCs were incubated with S-protein followed by mouse anti-myc antibody and goat anti-mouse IgG (RPE) (dotted lines). As controls, cells were not incubated with S-protein but were subsequently stained with mouse anti-myc antibody and goat anti-mouse IgG (solid histograms). S-protein was also incubated with SP-D before incubation with the cells (solid lines). (C) DCs and macrophages were stimulated for 6 h with LPS (0.5 μg/ml) or S-protein (20 μg/ml) in the presence of brefeldin A (10 μg/ml). The cells were fixed, permeabilized, and then stained with RPE-labelled mouse anti-TNF-α antibody (solid lines) or, as controls, with isotype mouse IgG (soild histograms). The cells were then analyzed by flow cytometry.

induction of TNF-α (Fig. 5C), but were not activated by S-protein. It is not clear whether S-protein activates macrophages through ACE2, which is expressed on

macrophages but not on DCs. Cytokine production by DCs and macrophages, upon S-protein stimulation, was also examined by ELISA. As shown in Fig. 6, while S-protein was consistently a weaker stimulus than LPS, it induced IL-6, IL-8 as well as TNF-α from macrophages. However, it did not induce significant cytokines from DCs. This is seemingly in contrast with the reported cytokine induction from DCs by live SARS-CoV virus (Law et al., 2005). However, it should be noted that live SARS-CoV are a more complex stimulus which could activate more complex signaling than S-protein in these cells. Nonetheless, the ability of S-protein to activate macrophages may contribute to the pathology of SARS through excessive pulmonary inflammation.

Discussion

SARS-CoV infects human hosts through the respiratory system and its interplay with the host innate immune system in the lung alveoli is likely to exert a major influence on the outcome of SARS-CoV infection. At the air–epithelial interfaces of lung alveoli, a surfactant monolayer is present. A primary function of the surfactant is to reduce surface tension at the end of expiration to prevent the collapse of the lung alveoli (Hawgood and Clements, 1990). It is also known that the surfactant contains two collectin molecules, i.e. SP-A and SP-D, which recognize carbohydrate structures on a wide range of microbial pathogens leading to killing and clearance of these microbes (Lu et al., 2002; Holmskov et al., 2003). Coronaviruses infect host cells through the highly glycosylated surface S-proteins. We therefore decided to investigate whether and how the carbohydrate structures on S-protein may interact with these surfactant collectins. To preserve the natural carbohydrate moiety on S-protein, it was expressed in eukaryotic cells. S-protein was expressed without the transmembrane and internal domains to permit its secretion into the medium and allow its purification as a soluble probe. To express S-protein as a trimer, its C-terminus was fused with the 'neck' sequence of SP-D, which is known to form strong triple coiled-coils and to cluster associated structures into parallel trimers. This strategy was initially to reflect the multiplicity of S-protein on the virus but a recent report showed that SARS-CoV S-protein in fact forms trimers naturally (Li et al., 2006).

The SARS-CoV S-protein (accession no. NC_004718) contains 18 potential Asn-linked glycosylation sites. Our results suggested that these potential glycosylation sites are probably mostly occupied as the purified S-protein exhibited a molecular mass of ∼200 kDa which is ∼70 kDa larger than that expected from its amino acid sequence (1194 residues or ∼130 kDa). Blocking of
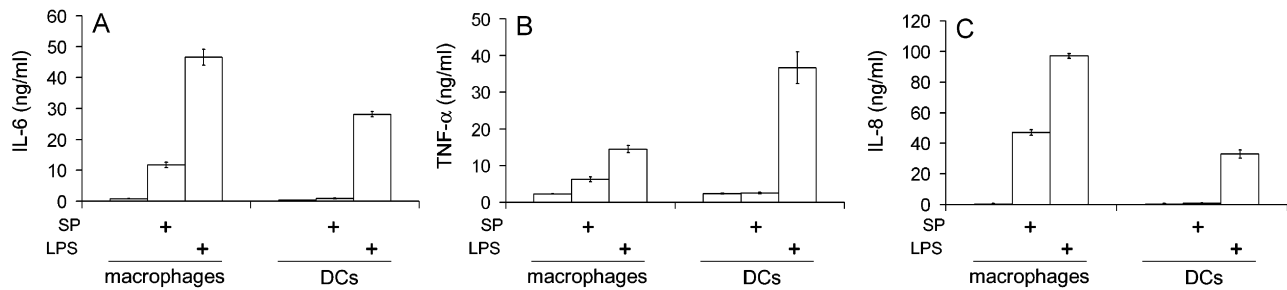
Fig. 6. Cytokine induction from DCs and macrophages by S-protein and LPS. DCs and macrophages were stimulated in 96-well plates with purified S-protein (SP, 20 μg/ml) or, as a control, LPS (0.5 μg/ml) for 24 h. IL-6 (A), TNF-α (B), and IL-8 (C) were measured in the media by ELISA using the DuoSet ELISA Development kits (R&D). The experiments were performed in triplicates and results were presented as means ± SD.

Asn-linked glycosylation with tunicamycin reduced S-protein to 130 kDa and completely prevented its secretion into the medium. This implies that glycosylation contributed to approx. one-third of the molecular mass of the purified S-protein and SARS-CoV replication requires proper S-protein glycosylation. The carbohydrate structures on S-protein might therefore represent a unique class of pathogen-associated molecular patterns (PAMPs) (Medzhitov and Janeway, 2000). Carbohydrate structures on many microorganisms are PAMPs that are recognized by host C-type lectins, including collectins (Sastry and Ezekowitz, 1993).

In the present study, we demonstrated that the pulmonary surfactant-associated collectin SP-D could bind to the SARS-CoV S-protein. The effective inhibition of SP-D-binding to S-protein by EDTA and sugars such as maltose and mannose suggest that SP-D binds to the carbohydrate moieties on S-protein. We similarly examined whether S-protein was recognized by SP-A, another surfactant-associated collectin. Due to the low level of binding detected, we were unable to conclude whether S-protein is also recognized by SP-A (data not shown). We showed that the serum collectin, MBL, was unable to recognize S-protein. One possible explanation for the apparently selective recognition of S-protein by SP-D may be that S-proteins display sugar residues that are preferentially recognized by SP-D. These two collectins exhibit different sugar specificity. For example, SP-D shows little affinity for GlcNAc to which MBL binds effectively (Lu et al., 1992; Holmskov et al., 2003). The disparities between SP-D and most other collectins in overall dimensions may also contribute to their differences in carbohydrate recognition. SP-D has long collagen-like helices which enable its CRDs to extend more than 90 nm apart whereas SP-A and MBL have much shorter collagen helices which can only extend their CRDs maximally less than 30 nm apart (Lu, 1997; Holmskov et al., 2003). C-type lectins, including collectins, mainly recognize specific sugar residues that are terminally presented and non-reducing (Lu et al.,

2002; Holmskov et al., 2003). While such sugar residues are common on extracellular microbial pathogens, viral glycoproteins are synthesized using the host eukaryotic cell machinery and most peripheral sugar residues are expected to be modified by terminal sialic acid residues. Therefore, despite the high degree of glycosylation of S-protein, suitable terminal sugar residues that are recognized by CRDs are probably infrequent and scattered. The much extended dimensions of SP-D, compared with MBL and SP-A, may enable it to bind to these scattered sugar residues more efficiently.

SARS is an acute pulmonary disease characterized by inflammation and immunological injury (Lang et al., 2003). Macrophages play essential roles in the onset and control of inflammation. S-protein is a major surface protein on SARS-CoV and we showed that S-protein binding to macrophages could activate the production of TNF-α from these cells. The observed macrophage activation by S-protein was not due to contamination of purified S-protein with microbial endotoxins since the purified S-protein showed no activation of TLR2 and TLR4 as judged using luciferase assays for NF-κB activation (data not shown) (Chen et al., 2004; Zhong et al., 2005). The purified S-protein showed no activation of DCs, also suggesting that the observed macrophage activation by purified S-protein is not due to contaminating microbial endotoxins as these microbial structures would also activate DCs. It is unclear how S-protein selectively activates macrophages but not DCs although it binds to both cell types. This may be attributed to the involvement of different receptors on the surface of these cells. For example, ACE2 is expressed on macrophages but not on DCs. However, soluble ACE2 was not available to verify whether this receptor was involved in the observed S-protein activation of macrophages.

While the mechanism by which S-protein activates macrophages is not clear, the ability of S-protein to induce TNF-α, IL-6 and IL-8 production in macrophages implies contributions of S-protein–macrophage interactions to the development of pulmonary

inflammation and tissue injury. It would be interesting to dissect the SARS-CoV S-protein and delineate the exact domain(s) that interact(s) with SP-D. The immunodominant sites on the S-protein of SARS-CoV have been identified (He et al., 2004), and neutralizing monoclonal antibodies that can protect ferrets against live SARS-CoV challenge have been developed (ter Meulen et al., 2004; van den Brink et al., 2005). These and our findings highlight the S-protein as a potential target for SARS-CoV vaccine development.

Acknowledgements

References

Cao, W., Tan, P., Lee, C.H., Zhang, H., Lu, J., 2006. A transforming growth factor β induced protein stimulates endocytosis and is up-regulated at the immature state of dendritic cells. Blood 107, 2777–2785.

Cavanagh, D., 1995. The coronavirus surface glycoprotein. In: Siddell, S.G. (Ed.), The Coronaviridae. Plenum Press, New York, pp. 73–113.

Cavanagh, D., Davis, P.J., Darbyshire, J.H., Peters, R.W., 1986. Coronavirus IBV: virus retaining spike glycopolypeptide S2 but not S1 is unable to induce virus-neutralizing or haemagglutination-inhibiting antibody, or induce chicken tracheal protection. J. Gen. Virol. 67, 1435–1442.

Chen, K., Lu, J., Wang, L., Gan, Y.H., 2004. Mycobacterial heat shock protein 65 enhances antigen cross-presentation in dendritic cells independent of Toll-like receptor 4 signaling. J. Leukocyte Biol. 75, 260–266.

Crouch, E., Wright, J.R., 2001. Surfactant proteins A and D and pulmonary host defense. Annu. Rev. Physiol. 63, 521–554.

Drosten, C., Gunther, S., Preiser, W., van der Werf, S., Brodt, H.R., Becker, S., Rabenau, H., Panning, M., Kolesnikova, L., Fouchier, R.A., Berger, A., Burguiere, A.M., Cinatl, J., Eickmann, M., Escriou, N., Grywna, K., Kramme, S., Manuguerra, J.C., Muller, S., Rickerts, V., Sturmer, M., Vieth, S., Klenk, H.D., Osterhaus, A.D., Schmitz, H., Doerr, H.W., 2003. Identification of a novel coronavirus in patients with severe acute respiratory syndrome. N. Engl. J. Med. 348, 1967–1976.

Enjuanes, L., Sola, I., Almazan, F., Ortego, J., Izeta, A., Gonzalez, J.M., Alonso, S., Sanchez, J.M., Escors, D., Calvo, E., Riquelme, C., Sanchez, C., 2001. Coronavirus derived expression systems. J. Biotechnol. 88, 183–204.

Fouchier, R.A., Kuiken, T., Schutten, M., van Amerongen, G., van Doornum, G.J., van den Hoogen, B.G., Peiris, M., Lim, W., Stohr, K., Osterhaus, A.D., 2003. Aetiology: Koch's postulates fulfilled for SARS virus. Nature 423, 240.

Gallagher, T.M., Buchmeier, M.J., 2001. Coronavirus spike proteins in viral entry and pathogenesis. Virology 279, 371–374.

Hawgood, S., Clements, J.A., 1990. Pulmonary surfactant and its apoproteins. J. Clin. Invest. 86, 1–6.

He, Y., Zhou, Y., Wu, H., Luo, B., Chen, J., Li, W., Jiang, S., 2004. Identification of immunodominant sites on the spike protein of severe acute respiratory syndrome (SARS) coronavirus: implication for developing SARS diagnostics and vaccines. J. Immunol. 173, 4050–4057.

Holmskov, U., Laursen, S.B., Malhotra, R., Wiedemann, H., Timpl, R., Stuart, G.R., Tornoe, I., Madsen, P.S., Reid, K.B.M., Jensenius, J.C., 1995. Comparative study of the structural and functional properties of a bovine plasma C-type lectin, collectin-43, with other collectins. Biochem. J. 305, 889–896.

Holmskov, U., Thiel, S., Jensenius, J.C., 2003. Collections and ficolins: humoral lectins of the innate immune defense. Annu. Rev. Immunol. 21, 547–578.

Hoppe, H.J., Barlow, P.N., Reid, K.B.M., 1994. A parallel three stranded alpha-helical bundle at the nucleation site of collagen triple-helix formation. FEBS Lett. 344, 191–195.

Jack, D.L., Klein, N.J., Turner, M.W., 2001. Mannose-binding lectin: targeting the microbial world for complement attack and opsonophagocytosis. Immunol. Rev. 180, 86–99.

Jeffers, S.A., Tusell, S.M., Gillim-Ross, L., Hemmila, E.M., Achenbach, J.E., Babcock, G.J., Thomas Jr., W.D., Thackray, L.B., Young, M.D., Mason, R.J., Ambrosino, D.M., Wentworth, D.E., Demartini, J.C., Holmes, K.V., 2004. CD209L (L-SIGN) is a receptor for severe acute respiratory syndrome coronavirus. Proc. Natl. Acad. Sci. USA 101, 15748–15753.

Ksiazek, T.G., Erdman, D., Goldsmith, C.S., Zaki, S.R., Peret, T., Emery, S., Tong, S., Urbani, C., Comer, J.A., Lim, W., Rollin, P.E., Dowell, S.F., Ling, A.E., Humphrey, C.D., Shieh, W.J., Guarner, J., Paddock, C.D., Rota, P., Fields, B., DeRisi, J., Yang, J.Y., Cox, N., Hughes, J.M., LeDuc, J.W., Bellini, W.J., Anderson, L.J., SARS Working Group, 2003. A novel coronavirus associated with severe acute respiratory syndrome. N. Engl. J. Med. 348, 1953–1966.

Kudo, K., Sano, H., Takahashi, H., Kuronuma, K., Yokota, S., Fujii, N., Shimada, K., Yano, I., Kumazawa, Y., Voelker, D.R., Abe, S., Kuroki, Y., 2004. Pulmonary collectins enhance phagocytosis of *Mycobacterium avium* through increased activity of mannose receptor. J. Immunol. 172, 7592–7602.

Kuiken, T., Fouchier, R.A., Schutten, M., Rimmelzwaan, G.F., van Amerongen, G., van Riel, D., Laman, J.D., de Jong, T., van Doornum, G., Lim, W., Ling, A.E., Chan, P.K., Tam, J.S., Zambon, M.C., Gopal, R., Drosten, C., van der Werf, S., Escriou, N., Manuguerra, J.C., Stohr, K., Peiris, J.S., Osterhaus, A.D., 2003. Newly discovered coronavirus as the primary cause of severe acute respiratory syndrome. Lancet 362, 263–270.

Lang, Z.W., Zhang, L.J., Zhang, S.J., Meng, X., Li, J.Q., Song, C.Z., Sun, L., Zhou, Y.S., Dwyer, D.E., 2003.

A linicopathological study of three cases of severe acute respiratory syndrome (SARS). Pathology 35, 526–531.

Law, H.K., Cheung, C.Y., Ng, H.Y., Sia, S.F., Chan, Y.O., Luk, W., Nicholls, J.M., Peiris, J.S., Lau, Y.L., 2005. Chemokine up-regulation in SARS-coronavirus-infected, monocyte-derived human dendritic cells. Blood 106, 2366–2374.

Lawson, P.R., Reid, K.B.M., 2000. The roles of surfactant proteins A and D in innate immunity. Immunol. Rev. 173, 66–78.

Leth-Larsen, R., Nordenbaek, C., Tornoe, I., Moeller, V., Schlosser, A., Koch, C., Teisner, B., Junker, P., Holmskov, U., 2003. Surfactant protein D (SP-D) serum levels in patients with community-acquired pneumonia small star, filled. Clin. Immunol. 108, 29–37.

LeVine, A.M., Whitsett, J.A., Gwozdz, J.A., Richardson, T.R., Fisher, J.H., Burhans, M.S., Korfhagen, T.R., 2000. Distinct effects of surfactant protein A or D deficiency during bacterial infection on the lung. J. Immunol. 165, 3934–3940.

Li, W., Moore, M.J., Vasilieva, N., Sui, J., Wong, S.K., Berne, M.A., Somasundaran, M., Sullivan, J.L., Luzuriaga, K., Greenough, T.C., Choe, H., Farzan, M., 2003. Angiotensin-converting enzyme 2 is a functional receptor for the SARS coronavirus. Nature 426, 450–454.

Li, F., Berardi, M., Li, W., Farzan, M., Dormitzer, P.R., Harrison, S.C., 2006. Conformational states of the severe acute respiratory syndrome coronavirus spike protein ectodomain. J. Virol. 80, 6794–6800.

Lu, J., 1997. Collectins: collectors of microorganisms for the innate immune system. Bioessays 19, 509–518.

Lu, J., Thiel, S., Wiedemann, H., Timpl, R., Reid, K.B.M., 1990. Binding of the pentamer/hexamer forms of mannan-binding protein to zymosan activates the proenzyme C1r2C1s2 complex, of the classical pathway of complement, without involvement of C1q. J. Immunol. 144, 2287–2294.

Lu, J., Willis, A.C., Reid, K.B.M., 1992. Purification, characterization and cDNA cloning of human lung surfactant protein D. Biochem. J. 284, 795–802.

Lu, J., Wiedemann, H., Holmskov, U., Thiel, S., Timpl, R., Reid, K.B.M., 1993. Structural similarity between lung surfactant protein D and conglutinin. Two distinct, C-type lectins containing collagen-like sequences. Eur. J. Biochem. 215, 793–799.

Lu, J., The, C., Kishore, U., Reid, K.B.M., 2002. Collectins and ficolins: sugar pattern recognition molecules of the mammalian innate immune system. Biochim. Biophys. Acta 1572, 387–400.

Luo, Z., Matthews, A.M., Weiss, S.R., 1999. Amino acid substitutions within the leucine zipper domain of the murine coronavirus spike protein cause defects in oligomerization and the ability to induce cell-to-cell fusion. J. Virol. 73, 8152–8159.

Madsen, J., Kliem, A., Tornoe, I., Skjodt, K., Koch, C., Holmskov, U., 2000. Localization of lung surfactant protein D on mucosal surfaces in human tissues. J. Immunol. 164, 5866–5870.

Marzi, A., Gramberg, T., Simmons, G., Moller, P., Rennekamp, A.J., Krumbiegel, M., Geier, M., Eisemann, J., Turza, N., Saunier, B., Steinkasserer, A., Becker, S., Bates, P., Hofmann, H., Pohlmann, S., 2004. DC-SIGN and DC-SIGNR interact with the glycoprotein of Marburg virus and the S protein of severe acute respiratory syndrome coronavirus. J. Virol. 78, 12090–12095.

Medzhitov, R., Janeway Jr., C., 2000. Innate immune recognition: mechanisms and pathways. Immunol. Rev. 173, 89–97.

Sastry, K., Ezekowitz, R.A., 1993. Collectins: pattern recognition molecules involved in first line host defense. Curr. Opin. Immunol. 5, 59–66.

Shi, L., Takahashi, K., Dundee, J., Shahroor-Karni, S., Thiel, S., Jensenius, J.C., Gad, F., Hamblin, M.R., Sastry, K.N., Ezekowitz, R.A., 2004. Mannose-binding lectin-deficient mice are susceptible to infection with *Staphylococcus aureus*. J. Exp. Med. 199, 1379–1390.

Strong, P., Kishore, U., Morgan, C., Lopez Bernal, A., Singh, M., Reid, K.B.M., 1998. A novel method of purifying lung surfactant proteins A and D from the lung lavage of alveolar proteinosis patients and from pooled amniotic fluid. J. Immunol. Methods 220, 139–149.

Super, M., Thiel, S., Lu, J., Levinsky, R.J., Turner, M.W., 1989. Association of low levels of mannan-binding protein with a common defect of opsonisation. Lancet 2, 1236–1239.

ter Meulen, J., Bakker, A.B., van den Brink, E.N., Weverling, G.J., Martina, B.E., Haagmans, B.L., Kuiken, T., de Kruif, J., Preiser, W., Spaan, W., Gelderblom, H.R., Goudsmit, J., Osterhaus, A.D., 2004. Human monoclonal antibody as prophylaxis for SARS coronavirus infection in ferrets. Lancet 363, 2139–2141.

van den Brink, E.N., Ter Meulen, J., Cox, F., Jongeneelen, M.A., Thijsse, A., Throsby, M., Marissen, W.E., Rood, P.M., Bakker, A.B., Gelderblom, H.R., Martina, B.E., Osterhaus, A.D., Preiser, W., Doerr, H.W., de Kruif, J., Goudsmit, J., 2005. Molecular and biological characterization of human monoclonal antibodies binding to the spike and nucleocapsid proteins of severe acute respiratory syndrome coronavirus. J. Virol. 79, 1635–1644.

Voss, T., Eistetter, H., Schafer, K.P., Engel, J., 1988. Macromolecular organization of natural and recombinant lung surfactant protein SP 28-36. Structural homology with the complement factor C1q. J. Mol. Biol. 201, 219–227.

Weis, W.I., Drickamer, K., 1994. Trimeric structure of a C-type mannose-binding protein. Structure 2, 1227–1240.

Weis, W.I., Taylor, M.E., Drickamer, K., 1998. The C-type lectin superfamily in the immune system. Immunol. Rev. 163, 19–34.

Zhong, F., Cao, W., Chan, E., Tay, P.N., Cahya, F.F., Zhang, H., Lu, J., 2005. Deviation from major codons in the toll-like receptor genes is associated with low toll-like receptor expression. Immunology 114, 83–93.